

On the eigenvalues of Toeplitz matrices with two off-diagonals

Sven-Erik Ekström*
sven-erik.ekstrom@it.uu.se

David Meadon*
david.meadon@it.uu.se

Abstract

Consider the Toeplitz matrix $T_n(f)$ generated by the symbol $f(\theta) = \hat{f}_r e^{ir\theta} + \hat{f}_0 + \hat{f}_{-s} e^{-is\theta}$, where $\hat{f}_r, \hat{f}_0, \hat{f}_{-s} \in \mathbb{C}$ and $0 < r < n$, $0 < s < n$. For $r = s = 1$ we have the classical tridiagonal Toeplitz matrices, for which the eigenvalues and eigenvectors are known. Similarly, the eigendecompositions are known for $1 < r = s$, when the generated matrices are “symmetrically sparse tridiagonal”.

In the current paper we study the eigenvalues of $T_n(f)$ for $1 < r < s$, which are “non-symmetrically sparse tridiagonal”. We propose an algorithm which constructs one or two ad hoc matrices smaller than $T_n(f)$, whose eigenvalues are sufficient for determining the full spectrum of $T_n(f)$. The algorithm is explained through use of a conjecture for which examples and numerical experiments are reported for supporting it and for clarifying the presentation. Open problems are briefly discussed.

Keywords: Toeplitz matrix sequences, eigenvalues, tridiagonal

MSC: 15A18, 15B05, 65F15

1 Introduction

We say that a function $f \in L^1(-\pi, \pi)$ generates a Toeplitz matrix $T_n(f) \in \mathbb{C}^{n \times n}$ if

$$T_n(f) = [\hat{f}_{i-j}]_{i,j=1}^n = \begin{bmatrix} \hat{f}_0 & \hat{f}_{-1} & \hat{f}_{-2} & \cdots & \hat{f}_{1-n} \\ \hat{f}_1 & \hat{f}_0 & \hat{f}_{-1} & \ddots & \vdots \\ \hat{f}_2 & \ddots & \ddots & \ddots & \vdots \\ \vdots & \ddots & \ddots & \ddots & \hat{f}_{-1} \\ \hat{f}_{n-1} & \cdots & \cdots & \hat{f}_1 & \hat{f}_0 \end{bmatrix},$$

where \hat{f}_k are the Fourier coefficients of f ,

$$\hat{f}_k = \frac{1}{2\pi} \int_{-\pi}^{\pi} f(\theta) e^{-ik\theta} d\theta, \quad \mathbf{i}^2 = -1, \quad k \in \mathbb{Z}.$$

The function f is called the generating symbol and is also a symbol for the singular value distribution in the Weyl sense, according to classical results by Szegő [36], Avram [1], Parter [27], Böttcher [14], Silbermann [14], Tilli [37], Tyrtshnikov [40], Serra-Capizzano [30, 31]. Furthermore, under specific assumptions, the generating function is the eigenvalue distribution symbol as well [2, 11, 25, 38]. Further spectral results of extremal type are in [9, 32], while we refer to the book by Garoni and Serra-Capizzano [24] for a general account on Toeplitz-like matrix-sequences, variable coefficient generalizations, and several applications.

In this article we focus on the spectrum of Toeplitz matrices generated by symbols of the form

$$f(\theta) = \hat{f}_0 + \hat{f}_r e^{ir\theta} + \hat{f}_{-s} e^{-is\theta}, \quad (1)$$

where $\theta \in [-\pi, \pi]$, $r, s \in \mathbb{Z}^+$, $r \neq s$, $\hat{f}_r, \hat{f}_0, \hat{f}_{-s} \in \mathbb{C}$ and $\hat{f}_r, \hat{f}_{-s} \neq 0$. Without loss of generality we take $r < s$ (since, if $r > s$, we can instead study the transposed matrix generated by $f(-\theta)$). The generated Toeplitz

*Department of Information Technology, Uppsala University

2 Main Results

The main result of this article is the following conjecture, with the rest of the article dedicated to supporting it.

Conjecture 1 (The eigenvalues of Toeplitz matrices generated by $g_{r,s}(\theta)$). *Assume $g_{r,s}(\theta)$ is defined as in (4) (with $1 \leq r \leq s$). Then, we know that a subset of the eigenvalues $\lambda_j(T_n(g_{r,s}))$, for $j = 1, \dots, n$, are real and positive [29]; denote this subset of the eigenvalues as $\lambda_+(T_n(g_{r,s}))$. Then, the eigenvalues in $\lambda_+(T_n(g_{r,s}))$ are, for $\gamma = \gcd(r, s)$, given by*

$$\lambda_+(T_n(g_{r,s}))^\omega = \left(\bigcup_{k=0}^{\gamma-\beta_\gamma} \lambda_+(T_{n_\gamma}(g_{r_\gamma, s_\gamma})) \right) \cup \left(\bigcup_{k=0}^{\beta_\gamma} \lambda_+(T_{n_\gamma+1}(g_{r_\gamma, s_\gamma})) \right) \quad (6)$$

where the parameters $\gamma, \omega, \beta_\gamma, n_\gamma$, and r_γ, s_γ , are defined in (7), (8), (15), (16), and (17). The eigenvalues $\lambda_+(T_{n_\gamma}(g_{r_\gamma, s_\gamma}))$ (and $\lambda_+(T_{n_\gamma+1}(g_{r_\gamma, s_\gamma}))$) are exactly the same as those of a smaller matrix $B_{(n_\gamma)\sigma}^{n_\gamma, r_\gamma, s_\gamma}$ (and $B_{(n_\gamma+1)\sigma}^{n_\gamma+1, r_\gamma, s_\gamma}$), possibly with multiplicity; a construction of these matrices is presented in Section 2.3.

The full spectrum of $T_n(g_{r,s})$ can be constructed by ω rotations of $\lambda_+(T_n(g_{r,s}))$ plus n_0 zero eigenvalues; see Section 2.4 and (11).

Hence, to summarise, we claim in Conjecture 1 that the positive real eigenvalues of a matrix $T_n(g_{r,s})$, where $1 \leq r \leq s$, are the same as the ω :th root of the eigenvalues of a non-unique other matrix (or two, with specified multiplicity) which we can construct automatically. The full spectrum of $T_n(g_{r,s})$ can then be constructed by rotations of these positive real eigenvalues, plus possibly n_0 zeros.

2.1 Properties of $\lambda_j(T_n(g_{r,s}))$ for $j = 1, \dots, n$

It is known that the eigenvalues of $T_n(g_{r,s})$, denoted $\lambda_j(T_n(g_{r,s}))$ for $j = 1, \dots, n$, lie in the convex hull of the essential range of the generating symbol $g_{r,s}(\theta)$; see, e.g., [9, 10, 24, 32], and the references therein. This fact is visualised in Figure 1, for three different parameters $\{n, r, s\}$.

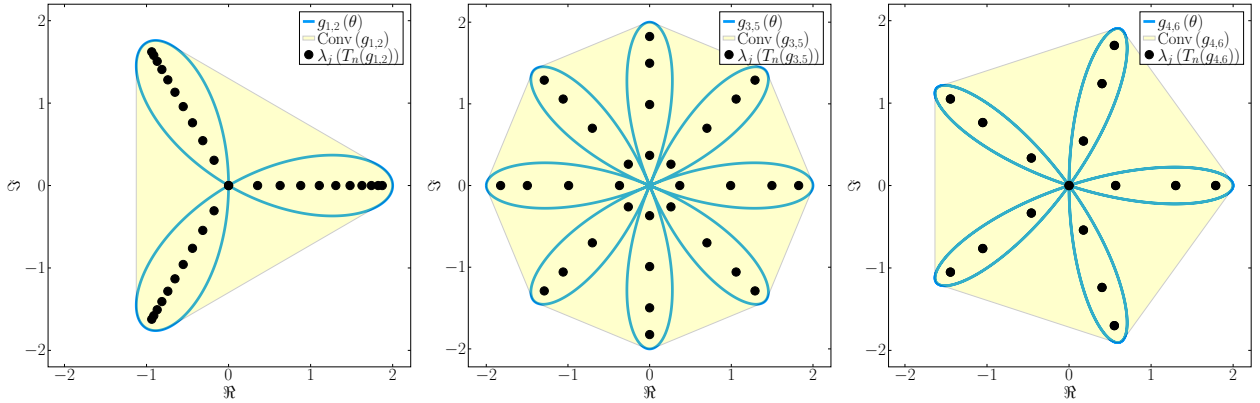


Figure 1: Symbol $g_{r,s}(\theta)$, the convex hull $\text{Conv}(g_{r,s})$ and the eigenvalues $\lambda_j(T_n(g_{r,s}))$, for $j = 1, \dots, n$. Parameters $\{n, r, s\}$. **Left:** $\{32, 1, 2\}$. **Middle:** $\{32, 3, 5\}$. **Right:** $\{32, 4, 6\}$.

The symbols $g_{r,s}$, and thus the eigenvalues $\lambda_j(T_n(g_{r,s}))$ for $j = 1, \dots, n$ lie in a “star” formation, for example see [11, pp. 204–205, p. 275], with ω distinct “arms”, where

$$\gamma = \gcd(r, s), \quad (7)$$

$$\sigma = r + s,$$

$$\omega = \frac{\sigma}{\gamma}, \quad (8)$$

$$\beta_\sigma = \text{mod}(n, \sigma), \quad (9)$$

$$n_\sigma = \frac{n - \beta_\sigma}{\sigma}. \quad (10)$$

The matrix $T_n(g_{r,s})$ has a total of

$$n_0 = (\gamma - \beta_\gamma) \text{mod}(n_\gamma, \omega) + \beta_\gamma \text{mod}(n_\gamma + 1, \omega), \quad (11)$$

zero eigenvalues, and in each distinct arm we have a total of $\frac{n-n_0}{\omega}$ non-zero eigenvalues. In the three panels of Figure 1 we have respectively two, none, and two zero eigenvalues. Generally we have that arm α is generated by $g_{r,s}(\frac{\theta}{\sigma} + \alpha\frac{2\pi}{\sigma})$ where $\alpha = 0$ corresponds to the arm that covers the positive real axis [29], $\alpha = 1$ is the next arm anti-clockwise, etc.; see Figure 2 for a visual reference.

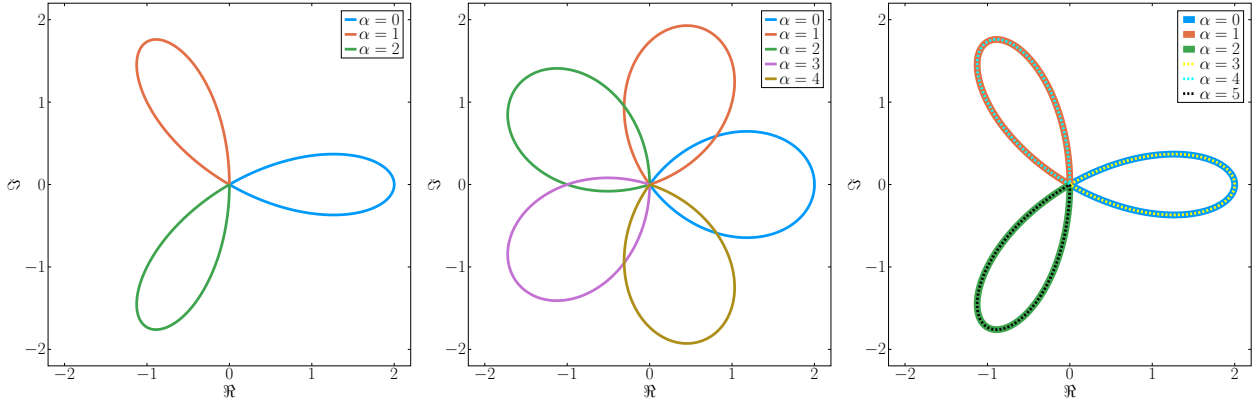


Figure 2: Symbol $g_{r,s}(\theta)$, with the different arms $\alpha = 0, \dots, \sigma - 1$ highlighted (number of distinct arms is ω). Parameters $\{r, s\}$. **Left:** $\{1, 2\}$ where $\omega = \sigma = 3$. **Middle:** $\{1, 4\}$ where $\omega = \sigma = 5$. **Right:** $\{2, 4\}$ where $\omega = 3$ and $\sigma = 6$.

2.2 Properties of $\lambda_+(T_n(g_{r,s}))$

It is reported in [11, 29], referring to results in [5], that there is one arm of the star, formed by the symbol $g_{r,s}$, that covers a part of the positive real axis. The eigenvalues $\lambda_j(T_n(g_{r,s}))$ in this arm are positive and real-valued. Denote the set of positive real-valued eigenvalues $\lambda_+(T_n(g_{r,s}))$, and we know from [29] that

$$0 < \lambda_+(T_n(g_{r,s})) \leq R = \frac{\sigma}{r^{\frac{r}{\sigma}} s^{\frac{s}{\sigma}}}.$$

Note that we here exclude the zero eigenvalues, which are of multiplicity n_0 , defined in (11). The non-zero eigenvalues of the other arms are rotations of $\lambda_+(T_n(g_{r,s}))$; see [29]. Now define the following function for the arm covering the eigenvalues $\lambda_+(T_n(g_{r,s}))$

$$a_{r,s}(\theta) = g_{r,s}\left(\frac{\theta}{\sigma}\right) = e^{i\frac{r}{\sigma}\theta} + e^{-i\frac{s}{\sigma}\theta}.$$

We notice that we do not have integer exponents, but if we construct the following symbol from $a_{r,s}(\theta)$,

$$b_{r,s}(\theta) = a_{r,s}(\theta)^\sigma = e^{ir\theta} (1 + e^{-i\theta})^\sigma, \quad (12)$$

we have a standard symbol for generated Toeplitz or Toeplitz-like matrices.

Remark 2. We note that Toeplitz matrices $T_n(b_{r,s})$, generated by the symbol $b_{r,s}(\theta)$ in (12), are non-symmetric, but have only real eigenvalues [33]. That is, the symbol $b_{r,s}$ is complex valued, and we have $\{T_n(b_{r,s})\} \sim_{\text{GLT}, \sigma} b_{r,s}$ and $\{T_n(b_{r,s})\} \sim_\lambda \mathbf{b}_{r,s}$, where $\mathbf{b}_{r,s}$ is real valued, see [33, Section 4.3],

$$\mathbf{b}_{r,s}(\theta) = \frac{\sin^\sigma(\theta)}{\sin^r(\frac{r}{\sigma}\theta) \sin^s(\frac{s}{\sigma}\theta)}. \quad (13)$$

See the theory of generalised locally Toeplitz (GLT) sequences [24] where we can deduce that also Toeplitz-like matrices B_n with the symbol $b_{r,s}(\theta)$ are $\{B_n\} \sim_{\text{GLT}, \sigma} b_{r,s}$ and $\{B_n\} \sim_\lambda \mathbf{b}_{r,s}$ (except for possibly $o(n)$ outliers, which are not present in the current setting of this article).

Furthermore, it is possible to rewrite the symbol $b_{r,s}(\theta)$ in (12) as a product of symbols

$$b_{r,s}(\theta) = c(\theta)^r c(-\theta)^s \quad (14)$$

where

$$c(\theta) = 1 + e^{i\theta}.$$

The fundamental idea of Conjecture 1 is that we can construct a matrix with symbol $b_{r,s}$ (or two with symbol $b_{r,\gamma,s,\gamma}$) of size smaller than n , whose eigenvalues (possibly with multiplicity) are exactly the eigenvalues $\lambda_+(T_n(g_{r,s}))$ to the power of ω .

2.3 Computing $\lambda_+(T_n(g_{r,s}))$

We now detail how to compute the positive real eigenvalues of $T_n(g_{r,s})$. In the case $\gamma = 1$, many parts of the ideas described below will simplify, however we here present the general case of $\gamma > 1$. When $\gamma > 1$, we will have a number of non-zero eigenvalues with multiplicity larger than one, and we can then look at a “reduced” case which yields the eigenvalues we seek. First define the following variables

$$\beta_\gamma = \text{mod}(n, \gamma), \quad (15)$$

$$n_\gamma = \frac{n - \beta_\gamma}{\gamma}, \quad (16)$$

$$r_\gamma = \frac{r}{\gamma}, \quad s_\gamma = \frac{s}{\gamma} \quad (17)$$

$$\sigma_\gamma = r_\gamma + s_\gamma = \omega. \quad (18)$$

Then, we use $\{n_\gamma, r_\gamma, s_\gamma\}$ as the new triple, that is, find the eigenvalues $\lambda_+(T_{n_\gamma}(g_{r_\gamma, s_\gamma}))$, by applying the algorithm as described in Section 2.3.1. We use the following notation for variables generated for the construction of the matrix $B_{(n_\gamma)_\sigma}^{n_\gamma, r_\gamma, s_\gamma}$

$$(\beta_\gamma)_\sigma = \text{mod}(n_\gamma, \sigma_\gamma), \quad (19)$$

$$(n_\gamma)_\sigma = \frac{n_\gamma - (\beta_\gamma)_\sigma}{\sigma_\gamma}. \quad (20)$$

After computing the positive real eigenvalues associated with this triple, we then repeat all the eigenvalues $\gamma - \beta_\gamma$ times.

However, if $\beta_\gamma > 0$ we also need to compute the eigenvalues for the triple $\{n_\gamma + 1, r_\gamma, s_\gamma\}$, that is, find the eigenvalues $\lambda_+(T_{n_\gamma+1}(g_{r_\gamma, s_\gamma}))$ where we compute the values in (19) and (20) using $n_\gamma + 1$ instead of n_γ . These eigenvalues are repeated β_γ times.

Thus, the full computation of $\lambda_+(T_n(g_{r,s}))$ is given by

$$\lambda_+(T_n(g_{r,s}))^\omega = \left(\bigcup_{k=0}^{\gamma-\beta_\gamma} \lambda_+(T_{n_\gamma}(g_{r_\gamma, s_\gamma})) \right) \cup \left(\bigcup_{k=0}^{\beta_\gamma} \lambda_+(T_{n_\gamma+1}(g_{r_\gamma, s_\gamma})) \right).$$

We will now present how to construct the matrices which has the same eigenvalues as $\lambda_+(T_{n_\gamma}(g_{r_\gamma, s_\gamma}))$, $\lambda_+(T_{n_\gamma+1}(g_{r_\gamma, s_\gamma}))$ or even all of $\lambda_+(T_n(g_{r,s}))$ in the case $\gamma = 1$. Thus, we may now assume that going forward the $\text{gcd}(r, s) = 1$, whether those be the original $\{r, s\}$ if $\gamma = 1$ or $\{r_\gamma, s_\gamma\}$ if we are working with the “reduced” case where $\gamma > 1$.

2.3.1 Construction of matrix $B_{n_\sigma}^{n, r, s}$

We propose that there exists a Toeplitz-like matrix, which we denote $B_{n_\sigma}^{n, r, s}$, which has the symbol $b_{r,s}(\theta)$ and has the eigenvalues $\bigcup_{j=1}^{n_\sigma} (\lambda_j(B_{n_\sigma}^{n, r, s}))^{\frac{1}{\sigma}} = \lambda_+(T_n(g_{r,s}))$. The matrix $B_{n_\sigma}^{n, r, s}$ is here uniquely defined by $\{n, r, s\}$ in the algorithm below (however, it is non-unique in sharing the eigenvalues with $\lambda_+(T_n(g_{r,s}))$, and can be constructed in many ways). The subscript n_σ , defined in (10), is only explicitly written to emphasise the size of the matrix; $n_\sigma < n$.

To construct a matrix $B_{n_\sigma}^{n, r, s}$ we use a prescribed, but non-unique, product of matrices of the form $T_{n_\sigma}(e^{-i\theta}c(\theta)^m)$ and their transposes; an implementation to generate these matrices is presented in Appendix A.4.

Remark 3. *The non-zero Fourier coefficients \hat{f}_k , $k = -1, \dots, m-1$ of the symbol $e^{-i\theta}c(\theta)^m = e^{-i\theta}(1 + e^{i\theta})^m$, used to generate the matrices $T_{n_\sigma}(e^{-i\theta}c(\theta)^m)$, are given by*

$$\hat{f}_k = \binom{m}{k+1}.$$

We provide here an algorithm to automatically generate the matrix $B_{n_\sigma}^{n, r, s}$. We begin by constructing two matrices $\mathcal{M}, \mathcal{P} \in \mathbb{Z}^{\sigma \times r}$ (defined in (23) and (24)). The elements of these matrices define how to generate $B_{n_\sigma}^{n, r, s}$,

$$B_{n_\sigma}^{n, r, s} = \prod_{k=1}^r T_{n_\sigma}^\top(e^{-i\theta}c(\theta)^{m_k}) (T_{n_\sigma}(e^{-i\theta}c(\theta)))^{p_k}, \quad (21)$$

$$= \prod_{k=1}^r T_{n_\sigma}(c(\theta)c(-\theta)^{m_k-1}) (T_{n_\sigma}(c(-\theta)))^{p_k}, \quad (22)$$

where $m_k = \mathcal{M}_{\beta+1,k}$ and $p_k = \mathcal{P}_{\beta+1,k}$. See Appendix A.2 for an implementation of (21). Furthermore, we have that the symbol of $B_{n_\sigma}^{n,r,s}$ in (22) will be

$$\begin{aligned} \{B_{n_\sigma}^{n,r,s}\}_{n_\sigma} &\sim_\sigma \prod_{k=1}^r c(\theta)c(-\theta)^{m_k-1}c(-\theta)^{p_k} \\ &= c(\theta)^r c(-\theta)^{\sum_{k=1}^r (m_k+p_k)-r} \\ &= \left[\sum_{k=1}^r (m_k+p_k) = \sigma \text{ by construction} \right] \\ &= c(\theta)^r c(-\theta)^s \\ &= b_{r,s}(\theta) \end{aligned}$$

as expected from (14). Note that all $\{B_{n_\sigma}^{n,r,s}\}_{n_\sigma} \sim_\lambda \mathbf{b}_{r,s}$.

Construction of matrices \mathcal{M} and \mathcal{P}

Defining $\tau = \text{mod}(s, r)$, then the elements of \mathcal{M} and \mathcal{P} are given by the following construction. The matrices $\mathcal{M}, \mathcal{P} \in \mathbb{Z}^{\sigma \times r}$ are both rectangular Toeplitz matrices defined by

$$\mathcal{M}_{i,j} = \begin{cases} 1, & \text{if } i = 1, \\ \mathcal{M}_{i-1,j} + 1, & \text{if } i > 1 \text{ and } \text{mod}(j-i, r) = \text{mod}(-1, r), \\ \mathcal{M}_{i-1,j}, & \text{otherwise,} \end{cases} \quad (23)$$

$$\mathcal{P}_{i,j} = \begin{cases} \frac{s-\tau}{r}, & \text{if } i = 1 \text{ and } j \leq r - \tau, \\ \frac{s-\tau}{r} + 1, & \text{if } i = 1 \text{ and } j > r - \tau, \\ \mathcal{P}_{i-1,j} - 1, & \text{if } i > 1 \text{ and } \text{mod}(j-i, r) = \text{mod}(r - \tau - 1, r), \\ \mathcal{P}_{i-1,j}, & \text{otherwise.} \end{cases} \quad (24)$$

An alternative, but equivalent, construction of \mathcal{M} and \mathcal{P} is presented in Appendix A.3. In the case that $r = 1$ then the matrices \mathcal{M} and \mathcal{P} are given as above, however if $r > 1$, then the columns of the matrices \mathcal{M} and \mathcal{P} in (23) and (24) need to be permuted and so will no longer have a Toeplitz structure. We create the permutation by first creating the ordered set $\mathcal{S}_\tau = (\tau, 2\tau, 3\tau, \dots, r\tau)$. Then, the permutation is defined as $p_{\text{perm}} = \text{mod}(\mathcal{S}_\tau, r)$ where the modulo operator is applied element-wise to the ordered set \mathcal{S}_τ , and instead of 0 for the final element (since it will be $\text{mod}(r\tau, r) = 0$) we will use r . Then, permute the columns of \mathcal{M} and \mathcal{P} with p_{perm} . See an implementation in Appendix A.3.

Erroneous perturbations when constructing $B_{n_\sigma}^{n,r,s}$

For $\beta_\sigma > s$ we will have that for some k in (22), p_k are negative; that is, inverses of $T_{n_\sigma}(c(-\theta))$ are used in the construction of $B_{n_\sigma}^{n,r,s}$. This results in incorrect and unwanted non-zero integer-valued perturbations being generated in the top right corner due to the inverted matrices; the generated $B_{n_\sigma}^{n,r,s}$ is in fact $B_{n_\sigma}^{n,r,s} + R_{n_\sigma}^{n,r,s}$ for odd n_σ and $B_{n_\sigma}^{n,r,s} - R_{n_\sigma}^{n,r,s}$ for even n_σ , where $R_{n_\sigma}^{n,r,s}$ is a low rank perturbation with strictly positive entries.

Our current approach to address this is to subtract these perturbations from the matrix and then proceed normally; that is, identify $R_{n_\sigma}^{n,r,s}$ and remove it. If the perturbations lie within the non-zero bandwidth of the correct matrix, we can construct a larger matrix where the perturbations are outside the bandwidth of the matrix, identify $R_{n_\sigma}^{n,r,s}$, and add or subtract it from the corresponding elements in the original sized (n_σ) matrix. See an implementation in Appendix A.2. However, this does not work in the case that the unwanted values cross over the main diagonal, and so we then have the restriction that $n > (r-1)\sigma$ rather than the essential restriction $n > s$. It is worth noting that by an informed search, a correct matrix $B_{n_\sigma}^{n,r,s}$ for $s < n \leq (r-1)\sigma$ can always manually be found, but an efficient algorithm to generate them has not yet been designed. We reiterate that this restriction on n is only necessary in the case that there are erroneous corner elements.

To exemplify these erroneous elements given by $R_{n_\sigma}^{n,r,s}$, that have to be removed when generating $B_{n_\sigma}^{n,r,s}$, see Section 3.4.

2.4 Constructing $\lambda_j(T_n(g_{r,s}))$ for $j = 1, \dots, n$ from $\lambda_+(T_n(g_{r,s}))$

Finally, we can then construct all the eigenvalues of $T_n(g_{r,s})$ from $\lambda_+(T_n(g_{r,s}))$ by

$$\begin{aligned} \lambda(T_n(g_{r,s})) &= \left(\bigcup_{\alpha=0}^{\omega-1} e^{2\pi i \frac{\alpha}{\omega}} \lambda_+(T_n(g_{r,s})) \right) \cup (\mathbf{0}_{n_0}) \\ &= \left[e^{2\pi i \frac{0}{\omega}}, e^{2\pi i \frac{1}{\omega}}, \dots, e^{2\pi i \frac{\omega-1}{\omega}} \right] \otimes \lambda_+(T_n(g_{r,s})) \cup (\mathbf{0}_{n_0}) \end{aligned}$$

where ω is as defined in (8), the multiplication of $e^{2\pi i \frac{\alpha}{\omega}}$, for $\alpha = 0, \dots, \omega - 1$, with $\lambda_+(T_n(g_{r,s}))$ is performed element-wise and $\mathbf{0}_{n_0}$ is a set of zeros of size n_0 defined in (11). An implementation is presented in Appendix A.6.

3 Examples and numerical experiments

3.1 Example 1: $\{r, s\} = \{1, 1\}$

As the first example we study the case $\{r, s\} = \{1, 1\}$, where we have a closed form formula for the eigenvalues for arbitrary n ; $\lambda_j(T_n(g_{1,1})) = 2 \cos\left(\frac{j\pi}{n+1}\right)$, for $j = 1, \dots, n$. In our algorithm, we have for $\{r, s\} = \{1, 1\}$ that

$$\mathcal{M} = \begin{bmatrix} 1 \\ 2 \end{bmatrix} \text{ and } \mathcal{P} = \begin{bmatrix} 1 \\ 0 \end{bmatrix}.$$

For $\beta_s = 0$, that is n is even, we have

$$B_{n/2}^{n,1,1} = \underbrace{\begin{bmatrix} 1 & & & & & \\ 1 & 1 & & & & \\ & \ddots & \ddots & & & \\ & & & 1 & 1 & \\ & & & & 1 & 1 \end{bmatrix}}_{T_{n/2}^\top(e^{-i\theta}c(\theta)^1)} \underbrace{\begin{bmatrix} 1 & 1 & & & & \\ & 1 & 1 & & & \\ & & \ddots & \ddots & & \\ & & & 1 & 1 & \\ & & & & 1 & \end{bmatrix}}_{T_{n/2}(e^{-i\theta}c(\theta)^1)} = \begin{bmatrix} 1 & 1 & & & & \\ 1 & 2 & 1 & & & \\ & \ddots & \ddots & \ddots & & \\ & & & 1 & 2 & 1 \\ & & & & 1 & 2 \end{bmatrix}.$$

Indicated in blue is the top left corner, the element which makes this matrix not a pure Toeplitz matrix. For this matrix we have $b_{1,1}(\theta) = 2 + 2 \cos(\theta)$ and $\lambda_j(B_{n/2}^{n,1,1}) = b_{1,1}(\theta_{j,n/2})$ where $\theta_{j,n/2} = \frac{j2\pi}{n+1}$, $j = 1, \dots, n/2$; see for example [8]. Thus, $\lambda_+(T_n(g_{1,1})) = \sqrt{b_{1,1}(\theta_{j,n/2})}$, and the full spectrum of $T_n(g_{1,1})$, as described in Section 2.4, is given by $\pm\lambda_+(T_n(g_{1,1}))$. Indeed, this is equivalent to the classical formula.

For $\beta_s = 1$, that is n is odd, we have one zero eigenvalue since $n_0 = 1$ in (11) and

$$B_{(n-1)/2}^{n,1,1} = \underbrace{\begin{bmatrix} 2 & 1 & & & & \\ 1 & 2 & 1 & & & \\ & \ddots & \ddots & \ddots & & \\ & & & 1 & 2 & 1 \\ & & & & 1 & 2 \end{bmatrix}}_{T_{(n-1)/2}^\top(e^{-i\theta}c(\theta)^2)} \underbrace{\begin{bmatrix} 1 & 1 & & & & \\ & 1 & 1 & & & \\ & & \ddots & \ddots & & \\ & & & 1 & 1 & \\ & & & & 1 & \end{bmatrix}}_{T_{(n-1)/2}(e^{-i\theta}c(\theta))^0} = \begin{bmatrix} 2 & 1 & & & & \\ 1 & 2 & 1 & & & \\ & \ddots & \ddots & \ddots & & \\ & & & 1 & 2 & 1 \\ & & & & 1 & 2 \end{bmatrix}.$$

We notice that this matrix is pure Toeplitz, with the same symbol $b_{1,1}(\theta)$ as above, but the eigenvalues $\lambda_+(T_n(g_{1,1})) = \sqrt{b_{1,1}(\theta_{j,(n-1)/2})}$ are now given by the grid $\theta_{j,(n-1)/2} = \frac{j2\pi}{n+1}$, $j = 1, \dots, (n-1)/2$. The eigenvalues of $T_n(g_{1,1})$ are given by $\pm\lambda_+(T_n(g_{1,1})) \cup 0$, and again this is equivalent to the classical formula.

3.2 Example 2: $\{r, s\} = \{1, 2\}$

As a second example we study the case $\{r, s\} = \{1, 2\}$. First we present the numerical difficulty of the non-symmetric eigenvalue problem visually in Figure 3. In the left panel we see the symbol $g_{1,2}(\theta)$ (blue) and the true eigenvalues $\lambda_j(T_{512}(g_{1,2}))$ (black) computed using high precision 256-bit BIGFLOAT data type in JULIA. Computing the spectrum using standard double precision, yields numerically unstable and incorrect results, presented as $\Psi_j(T_{512}(g_{1,2}))$ (red) and $\Psi_j(T_{512}^\top(g_{1,2}))$ (green). In the right panel we instead see the ϵ -pseudospectrum [10, 13, 14, 26, 28, 39], generated by the PSEUDOSPECTRA.JL [35] package, a JULIA implementation of the MATLAB toolbox EIGTOOL [42].

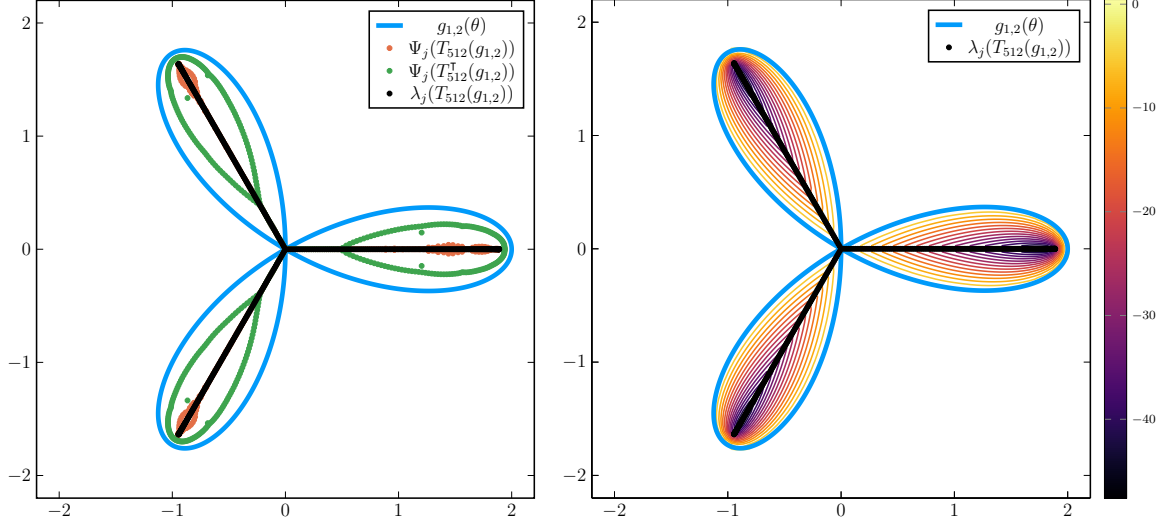


Figure 3: Spectra and pseudospectra, $\{n, r, s\} = \{512, 1, 2\}$: **Left:** Incorrect numerically computed eigenvalues $\Psi_j(T_{512}(g_{1,2}))$ and $\Psi_j(T_{512}^\top(g_{1,2}))$ using double precision and the correctly computed eigenvalues $\lambda_j(T_{512}(g_{1,2}))$ using 256-bit BIGFLOAT in JULIA. **Right:** The ϵ -pseudospectrum of $T_{512}(g_{1,2})$ computed using PSEUDOSPECTRA.JL, where each contour is a different $\log_{10}(\epsilon)$.

In our algorithm, we have for $\{r, s\} = \{1, 2\}$ that $\mathcal{M} = \begin{bmatrix} 1 \\ 2 \\ 3 \end{bmatrix}$ and $\mathcal{P} = \begin{bmatrix} 2 \\ 1 \\ 0 \end{bmatrix}$. Now, consider the three cases $n = \{15, 16, 17\}$, that is, $n_\sigma = 5$, and $\beta_\sigma = \{0, 1, 2\}$.

Below we present the three generated $B_5^{n,1,2}$, with the perturbations from the pure Toeplitz matrix $T_{n_\sigma}(b_{1,2})$ in top left corners indicated in blue.

$$\begin{aligned}
 B_5^{15,1,2} &= T_5^\top(e^{-i\theta}c(\theta)^1)T_5(e^{-i\theta}c(\theta))^2 = \begin{bmatrix} 1 & 0 & 0 & 0 & 0 \\ 1 & 1 & 0 & 0 & 0 \\ 0 & 1 & 1 & 0 & 0 \\ 0 & 0 & 1 & 1 & 0 \\ 0 & 0 & 0 & 1 & 1 \end{bmatrix} \begin{bmatrix} 1 & 1 & 0 & 0 & 0 \\ 0 & 1 & 1 & 0 & 0 \\ 0 & 0 & 1 & 1 & 0 \\ 0 & 0 & 0 & 1 & 1 \\ 0 & 0 & 0 & 0 & 1 \end{bmatrix}^2 = \begin{bmatrix} 1 & 2 & 1 & 0 & 0 \\ 1 & 3 & 3 & 1 & 0 \\ 0 & 1 & 3 & 3 & 1 \\ 0 & 0 & 1 & 3 & 3 \\ 0 & 0 & 0 & 1 & 3 \end{bmatrix}, \\
 B_5^{16,1,2} &= T_5^\top(e^{-i\theta}c(\theta)^2)T_5(e^{-i\theta}c(\theta))^1 = \begin{bmatrix} 2 & 1 & 0 & 0 & 0 \\ 1 & 2 & 1 & 0 & 0 \\ 0 & 1 & 2 & 1 & 0 \\ 0 & 0 & 1 & 2 & 1 \\ 0 & 0 & 0 & 1 & 2 \end{bmatrix} \begin{bmatrix} 1 & 1 & 0 & 0 & 0 \\ 0 & 1 & 1 & 0 & 0 \\ 0 & 0 & 1 & 1 & 0 \\ 0 & 0 & 0 & 1 & 1 \\ 0 & 0 & 0 & 0 & 1 \end{bmatrix}^1 = \begin{bmatrix} 2 & 3 & 1 & 0 & 0 \\ 1 & 3 & 3 & 1 & 0 \\ 0 & 1 & 3 & 3 & 1 \\ 0 & 0 & 1 & 3 & 3 \\ 0 & 0 & 0 & 1 & 3 \end{bmatrix}, \\
 B_5^{17,1,2} &= T_5^\top(e^{-i\theta}c(\theta)^3)T_5(e^{-i\theta}c(\theta))^0 = \begin{bmatrix} 3 & 3 & 1 & 0 & 0 \\ 1 & 3 & 3 & 1 & 0 \\ 0 & 1 & 3 & 3 & 1 \\ 0 & 0 & 1 & 3 & 3 \\ 0 & 0 & 0 & 1 & 3 \end{bmatrix} \begin{bmatrix} 1 & 1 & 0 & 0 & 0 \\ 0 & 1 & 1 & 0 & 0 \\ 0 & 0 & 1 & 1 & 0 \\ 0 & 0 & 0 & 1 & 1 \\ 0 & 0 & 0 & 0 & 1 \end{bmatrix}^0 = \begin{bmatrix} 3 & 3 & 1 & 0 & 0 \\ 1 & 3 & 3 & 1 & 0 \\ 0 & 1 & 3 & 3 & 1 \\ 0 & 0 & 1 & 3 & 3 \\ 0 & 0 & 0 & 1 & 3 \end{bmatrix}.
 \end{aligned}$$

The number of zero eigenvalues of $T_n(g_{1,2})$ are $n_0 = \{0, 1, 2\}$ for $n = \{15, 16, 17\}$ respectively. Furthermore, we can visualise how the eigenvalues change for different β_σ by looking at the characteristic polynomials $q_{n_\sigma}^{n,r,s}(x)$ for $B_{n_\sigma}^{n,r,s}$, that is $n = \{15, 16, 17\}$ for $\beta_\sigma = 0, 1, 2$, are

$$\begin{aligned}
 q_5^{15,1,2}(x) &= x^5 - 13x^4 + 55x^3 - 84x^2 + 35x - 1 \\
 q_5^{16,1,2}(x) &= x^5 - 14x^4 + 66x^3 - 120x^2 + 70x - 6 \\
 q_5^{17,1,2}(x) &= x^5 - 15x^4 + 78x^3 - 165x^2 + 126x - 21
 \end{aligned}$$

and the roots (which are the eigenvalues $\lambda_+(T_n(g_{1,2}))^\sigma$) are shown in Figure 4. The smallest eigenvalue is given by $q_5^{15,1,2}(x)$, that is, $\beta_\sigma = 0$, resulting in a larger condition number $\kappa(\cdot) = \frac{\sigma_{\max}}{\sigma_{\min}}$ than for $\beta_\sigma > 0$; $\kappa = \{242.8, 87.4, 38.3\}$. Also, we notice this pattern in Section 3.5, that the error and $\kappa(B_{n_\sigma}^{n,r,s})$ is declining as β_σ increases; See left panel in Figure 5.

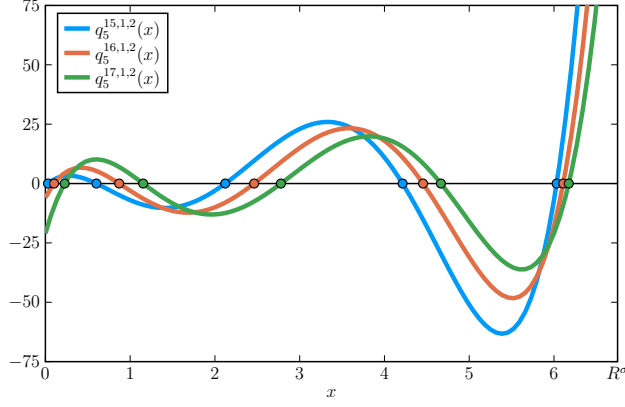


Figure 4: The characteristic polynomials $q_{n_\sigma}^{n,r,s}(x)$ for $B_{n_\sigma}^{n,r,s}$ with $n = \{15, 16, 17\}$, $\{r, s\} = \{1, 2\}$, and thus $\beta_\sigma = 0, 1, 2$. The roots are shown with circles. The positive real eigenvalues of $T_n(g_{1,2})$ are in the interval $(0, R)$, where $R^\sigma = \frac{\sigma^\sigma}{r^r s^s} = 6.75$.

The characteristic polynomials for $T_n(g_{r,s})$ are $p_n^{r,s}(x)$. As expected, we have

$$\begin{aligned} p_{15}^{1,2}(x) &= q_5^{15,1,2}(x^3), \\ p_{16}^{1,2}(x) &= xq_5^{16,1,2}(x^3), \\ p_{17}^{1,2}(x) &= x^2q_5^{17,1,2}(x^3), \end{aligned}$$

in accordance with Conjecture 1.

Remark 4. We note that R defined in [29, Section 7] to the power of σ is in this case defined by

$$R^\sigma = \frac{\sigma^\sigma}{r^r s^s} = \frac{3^3}{1^1 2^2} = \frac{27}{4} = 6.75,$$

so the upper bound of the real eigenvalues of $T_n(g_{1,2})$ is $R = 6.75^{\frac{1}{3}}$. For the general case of any $\{r, s\}$, and $\gamma = 1$, we have that $\mathfrak{b}_{r,s}$ in (13),

$$\lim_{\theta \rightarrow 0} \mathfrak{b}_{r,s}(\theta) = \lim_{\theta \rightarrow 0} \frac{\sin^\sigma(\theta)}{\sin^r(\frac{r}{\sigma}\theta) \sin^s(\frac{s}{\sigma}\theta)} = \lim_{\theta \rightarrow 0} \frac{(\frac{\sigma}{\sigma}\theta)^\sigma}{(\frac{r}{\sigma}\theta)^r (\frac{s}{\sigma}\theta)^s} = \frac{\sigma^\sigma}{r^r s^s} = R^\sigma,$$

since $\mathfrak{b}_{r,s}$ is even, and monotone in $[0, \pi]$, and has its maximum at $\theta = 0$.

3.3 Example 3: $\{r, s\} = \{2, 4\}$

For $\{r, s\} = \{2, 4\}$ we have that $\sigma = 6$, $\gamma = 2$, $\{r_\gamma, s_\gamma\} = \{1, 2\}$, and $\sigma_\gamma = 3$. Then for a given n , the eigenvalues of $T_n(g_{2,4})$ will be computed by using the union of the eigenvalues of $B_{(n_\gamma)_\sigma}^{n_\gamma, 1, 2}$ repeating them $\gamma - \beta_\gamma$ times and $B_{(n_\gamma+1)_\sigma}^{n_\gamma+1, 1, 2}$ repeated β_γ times. Take the cases $n = \{12, 13, 14, 15, 16, 17\}$, where the relevant variables have been computed in Table 1.

Table 1: Variables for Example 3.

n	β_σ	n_σ	β_γ	n_γ	$(\beta_\gamma)_\sigma$	$(n_\gamma)_\sigma$	$(n_\gamma + 1)_\sigma$	n_0
12	0	2	0	6	0	2	2	0
13	1	2	1	6	0	2	2	1
14	2	2	0	7	1	2	2	2
15	3	2	1	7	1	2	2	3
16	4	2	0	8	2	2	3	4
17	5	2	1	8	2	2	3	2

Thus, the necessary matrices to compute the eigenvalues are,

$$B_2^{6,1,2} = \begin{bmatrix} 1 & 2 \\ 1 & 3 \end{bmatrix}, \quad B_2^{7,1,2} = \begin{bmatrix} 2 & 3 \\ 1 & 3 \end{bmatrix}, \quad B_2^{8,1,2} = \begin{bmatrix} 3 & 3 \\ 1 & 3 \end{bmatrix}, \quad B_3^{9,1,2} = \begin{bmatrix} 1 & 2 & 1 \\ 1 & 3 & 3 \\ 0 & 1 & 3 \end{bmatrix}, \quad (25)$$

so, we compute the positive real eigenvalues using

$$\begin{aligned}\lambda_+(T_{12}(g_{2,4}))^3 &= \bigcup_{k=1}^2 \left(\bigcup_{j=1}^2 \lambda_j(B_2^{6,1,2}) \right), \\ \lambda_+(T_{13}(g_{2,4}))^3 &= \left(\bigcup_{j=1}^2 \lambda_j(B_2^{6,1,2}) \right) \cup \left(\bigcup_{j=1}^2 \lambda_j(B_2^{7,1,2}) \right), \\ \lambda_+(T_{14}(g_{2,4}))^3 &= \bigcup_{k=1}^2 \left(\bigcup_{j=1}^2 \lambda_j(B_2^{7,1,2}) \right), \\ \lambda_+(T_{15}(g_{2,4}))^3 &= \left(\bigcup_{j=1}^2 \lambda_j(B_2^{7,1,2}) \right) \cup \left(\bigcup_{j=1}^2 \lambda_j(B_2^{8,1,2}) \right), \\ \lambda_+(T_{16}(g_{2,4}))^3 &= \bigcup_{k=1}^2 \left(\bigcup_{j=1}^2 \lambda_j(B_2^{8,1,2}) \right), \\ \lambda_+(T_{17}(g_{2,4}))^3 &= \left(\bigcup_{j=1}^2 \lambda_j(B_2^{8,1,2}) \right) \cup \left(\bigcup_{j=1}^3 \lambda_j(B_3^{9,1,2}) \right),\end{aligned}$$

where the eigenvalues of the matrices (25) are either computed analytically or numerically. We see that in general we need to use a union of the eigenvalues of a total of γ matrices (where it is either one or two different ones) to compute the positive real eigenvalues of $T_n(g_{r,s})$.

In Table 2 is shown the characteristic polynomial of $T_n(g_{2,4})$ for $n = \{12, 13, 14, 15, 16, 17\}$ as well as the matrices constructed in (25).

Table 2: Characteristic polynomials of matrices in Example 3.

Matrix	Characteristic polynomial
$T_{12}(g_{2,4})$	$p_{12}^{2,4}(x) = x^{12} - 8x^9 + 18x^6 - 8x^3 + 1$
$T_{13}(g_{2,4})$	$p_{13}^{2,4}(x) = x(x^{12} - 9x^9 + 24x^6 - 17x^3 + 3)$
$T_{14}(g_{2,4})$	$p_{14}^{2,4}(x) = x^2(x^{12} - 10x^9 + 31x^6 - 30x^3 + 9)$
$T_{15}(g_{2,4})$	$p_{15}^{2,4}(x) = x^3(x^{12} - 11x^9 + 39x^6 - 48x^3 + 18)$
$T_{16}(g_{2,4})$	$p_{16}^{2,4}(x) = x^4(x^{12} - 12x^9 + 48x^6 - 72x^3 + 36)$
$T_{17}(g_{2,4})$	$p_{17}^{2,4}(x) = x^2(x^{15} - 13x^{12} + 58x^9 - 103x^6 + 66x^3 - 6)$
$B_2^{6,1,2}$	$q_2^{6,1,2}(x) = x^2 - 4x + 1$
$B_2^{7,1,2}$	$q_2^{7,1,2}(x) = x^2 - 5x + 3$
$B_2^{8,1,2}$	$q_2^{8,1,2}(x) = x^2 - 6x + 6$
$B_3^{9,1,2}$	$q_3^{9,1,2}(x) = x^3 - 7x^2 + 10x - 1$

We have from Table 2 and the number of zeros n_0 in Table 1,

$$\begin{aligned}p_{12}^{2,4}(x) &= q_2^{6,1,2}(x^3)q_2^{6,1,2}(x^3), \\ p_{13}^{2,4}(x) &= xq_2^{6,1,2}(x^3)q_2^{7,1,2}(x^3), \\ p_{14}^{2,4}(x) &= x^2q_2^{7,1,2}(x^3)q_2^{7,1,2}(x^3), \\ p_{15}^{2,4}(x) &= x^3q_2^{7,1,2}(x^3)q_2^{8,1,2}(x^3), \\ p_{16}^{2,4}(x) &= x^4q_2^{8,1,2}(x^3)q_2^{8,1,2}(x^3), \\ p_{17}^{2,4}(x) &= x^2q_2^{8,1,2}(x^3)q_3^{9,1,2}(x^3),\end{aligned}$$

As we are in the case $\beta_\sigma = 6, 7$, we have that $\beta_\sigma > s$, and thus we will have erroneous corner elements. In this setting, it is the last two rows of \mathcal{M} and \mathcal{P} that define the construction of $B_{n_\sigma}^{n,r,s}$, and includes negative values in \mathcal{P} . To get the correct $B_{n_\sigma}^{n,r,s}$ we replace the red elements on the right top corner with zeros.

$$\begin{aligned}
B_{10}^{86,3,5} - R_{10}^{86,3,5} &= T_{n_\sigma}^\top (e^{-i\theta} c(\theta)^3) T_{n_\sigma}^\top (e^{-i\theta} c(\theta)^3) (T_{n_\sigma} (e^{-i\theta} c(\theta)))^{-1} T_{n_\sigma}^\top (e^{-i\theta} c(\theta)^3) \\
&= \begin{bmatrix} 43 & 65 & 55 & 28 & 8 & 1 & 0 & 0 & 0 & -3 \\ 27 & 56 & 70 & 56 & 28 & 8 & 1 & 0 & 0 & -1 \\ 8 & 28 & 56 & 70 & 56 & 28 & 8 & 1 & 0 & 0 \\ 1 & 8 & 28 & 56 & 70 & 56 & 28 & 8 & 1 & 0 \\ 0 & 1 & 8 & 28 & 56 & 70 & 56 & 28 & 8 & 1 \\ 0 & 0 & 1 & 8 & 28 & 56 & 70 & 56 & 28 & 8 \\ 0 & 0 & 0 & 1 & 8 & 28 & 56 & 70 & 56 & 28 \\ 0 & 0 & 0 & 0 & 1 & 8 & 28 & 56 & 70 & 55 \\ 0 & 0 & 0 & 0 & 0 & 1 & 8 & 28 & 55 & 62 \\ 0 & 0 & 0 & 0 & 0 & 0 & 1 & 8 & 25 & 37 \end{bmatrix}, \\
B_{10}^{87,3,5} - R_{10}^{87,3,5} &= T_{n_\sigma}^\top (e^{-i\theta} c(\theta)^3) (T_{n_\sigma}^\top (e^{-i\theta} c(\theta)))^{-1} T_{n_\sigma}^\top (e^{-i\theta} c(\theta)^4) (T_{n_\sigma}^\top (e^{-i\theta} c(\theta)))^{-1} T_{n_\sigma}^\top (e^{-i\theta} c(\theta)^3) \\
&= \begin{bmatrix} 43 & 65 & 55 & 28 & 8 & 1 & 0 & 0 & -1 & -6 \\ 27 & 56 & 70 & 56 & 28 & 8 & 1 & 0 & 0 & -1 \\ 8 & 28 & 56 & 70 & 56 & 28 & 8 & 1 & 0 & 0 \\ 1 & 8 & 28 & 56 & 70 & 56 & 28 & 8 & 1 & 0 \\ 0 & 1 & 8 & 28 & 56 & 70 & 56 & 28 & 8 & 1 \\ 0 & 0 & 1 & 8 & 28 & 56 & 70 & 56 & 28 & 8 \\ 0 & 0 & 0 & 1 & 8 & 28 & 56 & 70 & 56 & 28 \\ 0 & 0 & 0 & 0 & 1 & 8 & 28 & 56 & 70 & 55 \\ 0 & 0 & 0 & 0 & 0 & 1 & 8 & 28 & 56 & 65 \\ 0 & 0 & 0 & 0 & 0 & 0 & 1 & 8 & 27 & 43 \end{bmatrix}.
\end{aligned}$$

We have thus identified the low rank matrix $R_{n_\sigma}^{n,r,s}$ (for all matrices $B_{n_\sigma}^{n,r,s}$ large enough with the same β_σ) and can use this to construct the correct $B_{n_\sigma}^{n,r,s}$ for smaller matrices; see the four examples below.

$$\begin{aligned}
B_4^{38,3,5} - R_4^{38,3,5} &= \begin{bmatrix} 43 & 65 & 55 & 25 \\ 27 & 56 & 70 & 54 \\ 8 & 28 & 55 & 62 \\ 1 & 8 & 25 & 37 \end{bmatrix} = \underbrace{\begin{bmatrix} 43 & 65 & 55 & 28 \\ 27 & 56 & 70 & 55 \\ 8 & 28 & 55 & 62 \\ 1 & 8 & 25 & 37 \end{bmatrix}}_{B_4^{38,3,5}} - \underbrace{\begin{bmatrix} 0 & 0 & 0 & 3 \\ 0 & 0 & 0 & 1 \\ 0 & 0 & 0 & 0 \\ 0 & 0 & 0 & 0 \end{bmatrix}}_{R_4^{38,3,5}} \\
B_4^{39,3,5} - R_4^{39,3,5} &= \begin{bmatrix} 43 & 65 & 54 & 22 \\ 27 & 56 & 70 & 54 \\ 8 & 28 & 56 & 65 \\ 1 & 8 & 27 & 43 \end{bmatrix} = \underbrace{\begin{bmatrix} 43 & 65 & 55 & 28 \\ 27 & 56 & 70 & 55 \\ 8 & 28 & 56 & 65 \\ 1 & 8 & 27 & 43 \end{bmatrix}}_{B_4^{39,3,5}} - \underbrace{\begin{bmatrix} 0 & 0 & 1 & 6 \\ 0 & 0 & 0 & 1 \\ 0 & 0 & 0 & 0 \\ 0 & 0 & 0 & 0 \end{bmatrix}}_{R_4^{39,3,5}}
\end{aligned}$$

Note that we add $R_{n_\sigma}^{n,r,s}$ from the originally constructed $B_{n_\sigma}^{n,r,s}$ to get the true $B_{n_\sigma}^{n,r,s}$, since $n_\sigma = 4$ is even.

$$\begin{aligned}
B_5^{46,3,5} + R_5^{46,3,5} &= \begin{bmatrix} 43 & 65 & 55 & 28 & 11 \\ 27 & 56 & 70 & 56 & 29 \\ 8 & 28 & 56 & 70 & 55 \\ 1 & 8 & 28 & 55 & 62 \\ 0 & 1 & 8 & 25 & 37 \end{bmatrix} = \underbrace{\begin{bmatrix} 43 & 65 & 55 & 28 & 8 \\ 27 & 56 & 70 & 56 & 28 \\ 8 & 28 & 56 & 70 & 55 \\ 1 & 8 & 28 & 55 & 62 \\ 0 & 1 & 8 & 25 & 37 \end{bmatrix}}_{B_5^{46,3,5}} + \underbrace{\begin{bmatrix} 0 & 0 & 0 & 0 & 3 \\ 0 & 0 & 0 & 0 & 1 \\ 0 & 0 & 0 & 0 & 0 \\ 0 & 0 & 0 & 0 & 0 \\ 0 & 0 & 0 & 0 & 0 \end{bmatrix}}_{R_5^{46,3,5}} \\
B_5^{47,3,5} + R_5^{47,3,5} &= \begin{bmatrix} 43 & 65 & 55 & 29 & 14 \\ 27 & 56 & 70 & 56 & 29 \\ 8 & 28 & 56 & 70 & 55 \\ 1 & 8 & 28 & 56 & 65 \\ 0 & 1 & 8 & 27 & 43 \end{bmatrix} = \underbrace{\begin{bmatrix} 43 & 65 & 55 & 28 & 8 \\ 27 & 56 & 70 & 56 & 28 \\ 8 & 28 & 56 & 70 & 55 \\ 1 & 8 & 28 & 56 & 65 \\ 0 & 1 & 8 & 27 & 43 \end{bmatrix}}_{B_5^{47,3,5}} + \underbrace{\begin{bmatrix} 0 & 0 & 0 & 1 & 6 \\ 0 & 0 & 0 & 0 & 1 \\ 0 & 0 & 0 & 0 & 0 \\ 0 & 0 & 0 & 0 & 0 \\ 0 & 0 & 0 & 0 & 0 \end{bmatrix}}_{R_5^{47,3,5}}
\end{aligned}$$

Note that we subtract $R_{n_\sigma}^{n,r,s}$ from the originally constructed $B_{n_\sigma}^{n,r,s}$ to get the true $B_{n_\sigma}^{n,r,s}$, since $n_\sigma = 5$ is odd.

3.5 Numerical experiments

Two sets of numerical experiments are performed to verify Conjecture 1. First, we have

$$\begin{aligned} r &= 1, \dots, 20, \\ s &= r, \dots, 20, \\ n &= \sigma^2 + \beta_\sigma, \quad \sigma = r + s, \quad \beta_\sigma = 0, \dots, \sigma - 1, \end{aligned}$$

that is, n grows as σ^2 , and the largest matrix is of size $n = 1639$. We compute $\lambda_j(T_n(g_{r,s}))$ using 256-bit `BigFloat` (machine epsilon $\varepsilon = \mathcal{O}(10^{-77})$) in `JULIA` with the package `GENERICSchur.jl` [34]. For select r and s were computed with 2048-bit precision for reference purposes. With same precision we compute $\lambda_+(T_n(g_{r,s}))$ using the proposed algorithm supporting Conjecture 1; algorithm implemented in Appendix A. We present here a subset of these results in the left panel of Figure 5, where we have plotted the error for $r = 5$, $s = \{6, \dots, 10\}$.

We define the error between the spectrum of $T_n(g_{r,s})$ computed using a standard solver and the presented algorithm as follows

$$\max_{j=1, \dots, n} \left| \left| \lambda_{\rho_1(j)}(T_n(g_{r,s}))_{\text{std}} \right| - \left| \lambda_{\rho_2(j)}(T_n(g_{r,s}))_{\text{alg}} \right| \right|,$$

where ρ_1 and ρ_2 are two permutations of $\{1, \dots, n\}$ that respectively sort the eigenvalues of the computations in ascending order by absolute value. Furthermore, only the non-zero eigenvalue error is shown, as if we include the zero eigenvalues, then the error becomes the magnitude of the zero eigenvalues computed by the standard solver which is much larger than the error of the non-zero eigenvalues.

We see that the general trend is for the error to decrease with β_σ , that is that $\beta_\sigma = 0$ will have the largest error; the condition number is also decreasing, exemplified earlier in Section 3.2 and Figure 4. Thus, in the second experiment which goes over a larger range of $\{r, s\}$ with a smaller n , we will only compute for $\beta_\sigma = 0$ as this will yield the largest error. The second experiment performed was

$$\begin{aligned} r &= 1, \dots, 50, \\ s &= r, \dots, 100, \\ n &= 3\sigma, \quad \sigma = r + s, \end{aligned}$$

where the largest matrix is $n = 450$. Computations are done with precisions $\{53, 256, 512, 1024, 2048\}$ -bit for the full matrix $T_n(g_{r,s})$ and the proposed algorithm where 53-bit is standard double precision (`FLOAT64`) and the 2048-bit solution of the full matrix $T_n(g_{r,s})$ is used as the reference solution. A subset of the results are shown in the right panel of Figure 5. We show here how the error changes for a fixed value of r ($r = 25$ in this case), while ranging $s = r, \dots, 100$. What we see is that the error increases as s increases for all precisions and this will be due to the ill-conditioned nature of the $B_{n_\sigma}^{n,r,s}$ matrices.

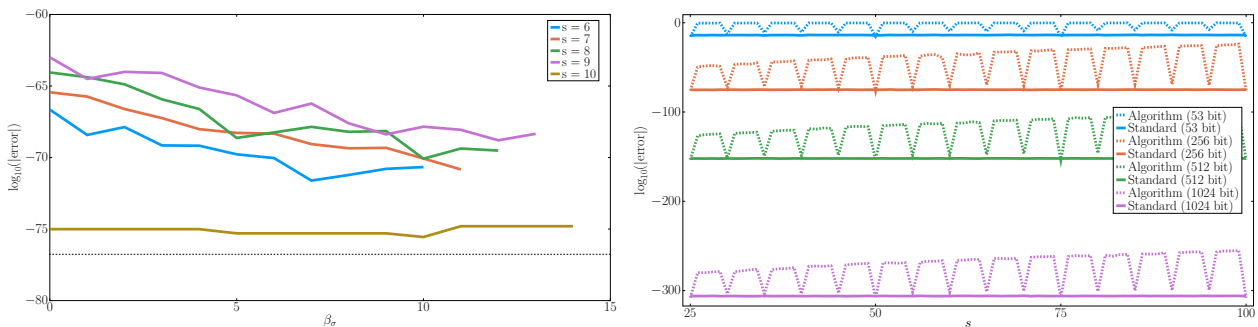


Figure 5: **Left:** Errors for $r = 5$ with varying $s = 6, \dots, 10$, $\beta_\sigma = 0, \dots, \sigma - 1$, and $n = \sigma^2 + \beta_\sigma$. Computed using 256-bit `BIGFLOAT` and compared to 2048-bit `BIGFLOAT`. Machine epsilon for 256-bit `BIGFLOAT` is $1.72 \cdot 10^{-77}$ (black dashed line). **Right:** Errors for $r = 25$ with varying $s = 25, \dots, 100$ and $n = \sigma^2$, that is, $\beta_\sigma = 0$. Both the algorithm and a standard eigenvalue solver is used for $T_{\sigma^2}(g_{25,s})$ for different precisions. Double precision (`FLOAT64`) is used for computations with 53-bit precision, and `BIGFLOAT` otherwise. Note the spikes down in the error when we have $\gamma > 1$.

An additional numerical consideration is that the elements of $B_{n_\sigma}^{n,r,s}$ can easily grow such that integer overflow is a concern; we use `INT128` as default in Appendix A but `BIGINT` may be used if this is an issue for large $\{n, r, s\}$. Presented below is $B_3^{231,38,39}$ where a standard 64-bit integer (`INT64`) would not work.

$$B_3^{231,38,39} = \begin{bmatrix} 2937189730080557577 & 9536995145808582886 & 11892438427558067162 \\ 6599805415728025309 & 21429433573366650048 & 26722066585196691901 \\ 5292633011830041853 & 17185071439388109015 & 21429433573366650048 \end{bmatrix}$$

The condition number of this matrix is $4.8 \cdot 10^{46}$, highlighting the need to use high precision data types when computing the eigenvalues, $\{1.0 \cdot 10^{-27}, 2.2 \cdot 10^7, 4.6 \cdot 10^{19}\}$.

The final numerical aspect that we mention is the computational time of the algorithm. See Table 3 which shows the minimal time used for the outlined algorithm in this paper and a standard eigenvalue solver (`eigvals` from `GENERICSCHUR.JL` in `JULIA`) for three different $\{n, r, s\}$ triples. The timings were performed on a computer with an AMD Epyc 7502P CPU (32 core, 1024 GB RAM) and `BENCHMARKTOOLS.JL` [15].

The timings show, especially in the experiment with $\{n, r, s\} = \{676, 7, 19\}$, that we can compute the eigenvalues of $T_n(g_{r,s})$ with much higher precision using the presented algorithm with a comparable or faster execution time than a `FLOAT64` computation of the full matrix (which will yield a considerable higher error). Optimizing the code in Appendix A, and using iterative refinement [16] we could probably increase the speed even further.

Table 3: Timings, in seconds, using the algorithm of this paper and a standard eigenvalue solver for three $\{n, r, s\}$ with different precisions. Standard double precision (`FLOAT64`) is used for 53-bit and `BIGFLOAT` for the other computations.

precision (bit)	$\{n, r, s\} = \{49, 2, 5\}$		$\{n, r, s\} = \{256, 4, 12\}$		$\{n, r, s\} = \{676, 7, 19\}$	
	Algorithm	Standard	Algorithm	Standard	Algorithm	Standard
53	0.00006	0.00055	0.00008	0.02654	0.00106	0.34084
64	0.00070	0.15268	0.00604	4.89205	0.01397	398.04027
128	0.00098	0.19567	0.00785	5.70696	0.01758	515.63287
256	0.00127	0.26923	0.01106	7.03421	0.02503	694.99100
512	0.00173	0.35154	0.01488	8.67083	0.03627	933.47496
1024	0.00284	0.60876	0.02403	14.36312	0.06258	1603.19599
2048	0.00577	1.23769	0.05347	23.06511	0.13496	2903.01721

4 Conclusions

Toeplitz matrices with two non-zero off-diagonals can be classified into three different cases. Firstly classical tridiagonal, and secondly “symmetrically sparse tridiagonal”; we have analytical expressions for the eigenvalues (and eigenvectors) of these matrices. In the third, more general case we have conjectured in Conjecture 1, and argued in this paper, that it is possible to generate all the eigenvalues by generating the positive real subset of the eigenvalues of the original matrix from one or two smaller matrices (possibly with multiplicity), and then by rotation in the complex plane, and possibly adding zeros.

Some aspects to further investigate, improve, and prove on the results of this paper are

- Prove Conjecture 1.
- Devise an algorithm which works also for small matrices, see the restriction in subsection 2.3. Also, there might be some approach that does not yield any erroneous corners, given by the low rank perturbation $R_{n_\sigma}^{n,r,s}$, at all.
- Devise an algorithm for computing the corresponding eigenvectors.
- The symbol $\mathfrak{b}_{r,s}$ in (13) is not used in this article, since we are interested in the exact spectrum, and we do not know (in the general case) a grid ξ_j , for $j = 1, \dots, n_\sigma$, such that $\lambda_j(B_{n_\sigma}^{n,r,s}) = \mathfrak{b}_{r,s}(\xi_j)$, for $j = 1, \dots, n_\sigma$; we do know this grid in Example 1 in Section 3. However, we could use the symbol $\mathfrak{b}_{r,s}(\theta)$ in conjunction with matrix-less methods [3, 6, 7, 12, 17, 18] to accurately and efficiently numerically approximate the spectrum of arbitrarily large n_σ . As an example, in [21] we indeed have shown that the matrix-less method works on the matrices in Example 2, for $\beta_\sigma = 2$.

5 Acknowledgements

The first author would like to thank Albrecht Böttcher for his inspirational works in the field of Toeplitz-like matrices, and welcoming and illuminating discussions in Chemnitz. We also thank Stefano Serra-Capizzano and Carlo Garoni for helpful suggestions for improving the paper. The research of the second author is in part financed by the Centre for Interdisciplinary Mathematics (CIM) at Uppsala University.

References

- [1] F. AVRAM, *On bilinear forms in Gaussian random variables and Toeplitz matrices*, Probability Theory and Related Fields, 79 (1988), pp. 37–45.
- [2] G. BARBARINO AND S. SERRA-CAPIZZANO, *Non-Hermitian perturbations of Hermitian matrix-sequences and applications to the spectral analysis of the numerical approximation of partial differential equations*, Numerical Linear Algebra with Applications, 27 (2020).
- [3] M. BARRERA, A. BÖTTCHER, S. M. GRUDSKY, AND E. A. MAXIMENKO, *Eigenvalues of even very nice Toeplitz matrices can be unexpectedly erratic*, in The Diversity and Beauty of Applied Operator Theory, Operator theory, Springer International Publishing, Cham, 2018, pp. 51–77.
- [4] J. BEZANSON, A. EDELMAN, S. KARPINSKI, AND V. B. SHAH, *Julia: A fresh approach to numerical computing*, SIAM Review, 59 (2017), pp. 65–98.
- [5] M. BIERNACKI, *Sur les équations algébriques contenant des paramètres arbitraires*, Bulletin L'Académie Polonaise des Science, (1928), pp. 541–685.
- [6] J. M. BOGOYA, A. BÖTTCHER, S. M. GRUDSKY, AND E. A. MAXIMENKO, *Eigenvalues of Hermitian Toeplitz matrices with smooth simple-loop symbols*, Journal of Mathematical Analysis and Applications, 422 (2015), pp. 1308–1334.
- [7] J. M. BOGOYA, S. M. GRUDSKY, AND E. A. MAXIMENKO, *Eigenvalues of Hermitian Toeplitz matrices generated by simple-loop symbols with relaxed smoothness*, in Large Truncated Toeplitz Matrices, Toeplitz Operators, and Related Topics, Operator theory, Springer International Publishing, Cham, 2017, pp. 179–212.
- [8] E. BOZZO AND C. DI FIORE, *On the use of certain matrix algebras associated with discrete trigonometric transforms in matrix displacement decomposition*, SIAM Journal on Matrix Analysis and Applications, 16 (1995), pp. 312–326.
- [9] A. BÖTTCHER AND S. M. GRUDSKY, *On the condition numbers of large semidefinite Toeplitz matrices*, Linear Algebra and its Applications, 279 (1998), pp. 285–301.
- [10] ———, *Toeplitz Matrices, Asymptotic Linear Algebra, and Functional Analysis*, Birkhäuser Basel, 2000.
- [11] ———, *Spectral Properties of Banded Toeplitz Matrices*, Society for Industrial and Applied Mathematics, 2005.
- [12] A. BÖTTCHER, S. M. GRUDSKY, AND E. A. MAKSIMENKO, *Inside the eigenvalues of certain Hermitian Toeplitz band matrices*, Journal of Computational and Applied Mathematics, 233 (2010), pp. 2245–2264.
- [13] A. BÖTTCHER, S. M. GRUDSKY, AND B. SILBERMANN, *Norms of inverses, spectra, and pseudospectra of large truncated Wiener-Hopf operators and Toeplitz matrices*, New York Journal of Mathematics, (1997), pp. 1—31.
- [14] A. BÖTTCHER AND B. SILBERMANN, *Introduction to large truncated Toeplitz matrices*, Universitext, Springer, New York, NY, 1999 ed., Dec. 2012.
- [15] J. CHEN AND J. REVELS, *Robust benchmarking in noisy environments*, arXiv e-prints, (2016).
- [16] J. J. DONGARRA, C. B. MOLER, AND J. H. WILKINSON, *Improving the accuracy of computed eigenvalues and eigenvectors*, SIAM Journal on Numerical Analysis, 20 (1983), pp. 23–45.
- [17] S.-E. EKSTRÖM AND C. GARONI, *A matrix-less and parallel interpolation–extrapolation algorithm for computing the eigenvalues of preconditioned banded symmetric Toeplitz matrices*, Numerical Algorithms, 80 (2018), pp. 819–848.
- [18] S.-E. EKSTRÖM, C. GARONI, AND S. SERRA-CAPIZZANO, *Are the eigenvalues of banded symmetric Toeplitz matrices known in almost closed form?*, Experimental Mathematics, 27 (2017), pp. 478–487.
- [19] S.-E. EKSTRÖM AND S. SERRA-CAPIZZANO, *Eigenvalues and eigenvectors of banded Toeplitz matrices and the related symbols*, Numerical Linear Algebra with Applications, 25 (2018), p. e2137.
- [20] ———, *Eigenpairs of some particular band Toeplitz matrices: A comment*, Numerical Linear Algebra with Applications, 27 (2020).

- [21] S.-E. EKSTRÖM AND P. VASSALOS, *A matrix-less method to approximate the spectrum and the spectral function of Toeplitz matrices with real eigenvalues*, Numerical Algorithms, 89 (2021), pp. 701–720.
- [22] C. M. FONSECA, *Eigenpairs of some particular band Toeplitz matrices: A comment*, Numerical Linear Algebra with Applications, 27 (2020).
- [23] F. GANTMAKHER AND M. KREIN, *Oscillation Matrices and Kernels and Small Vibrations of Mechanical Systems*, State Publishing House for Technical-Theoretical Literature, 1950.
- [24] C. GARONI AND S. SERRA-CAPIZZANO, *Generalized Locally Toeplitz Sequences: Theory and Applications (Volume 1)*, Springer International Publishing, 2017.
- [25] L. GOLINSKII AND S. SERRA-CAPIZZANO, *The asymptotic properties of the spectrum of nonsymmetrically perturbed Jacobi matrix sequences*, Journal of Approximation Theory, 144 (2007), pp. 84–102.
- [26] H. J. LANDAU, *On Szegő’s eigenvalue distribution theorem and non-Hermitian kernels*, Journal d’Analyse Mathématique, 28 (1975), pp. 335–357.
- [27] S. V. PARTER, *On the distribution of the singular values of Toeplitz matrices*, Linear Algebra and its Applications, 80 (1986), pp. 115–130.
- [28] L. REICHEL AND L. N. TREFETHEN, *Eigenvalues and pseudo-eigenvalues of Toeplitz matrices*, Linear Algebra and its Applications, 162–164 (1992), pp. 153–185.
- [29] P. SCHMIDT AND F. SPITZER, *The Toeplitz Matrices of an Arbitrary Laurent Polynomial.*, Mathematica Scandinavica, 8 (1960), pp. 15–38.
- [30] S. SERRA-CAPIZZANO, *Generalized locally Toeplitz sequences: spectral analysis and applications to discretized partial differential equations*, Linear Algebra and its Applications, 366 (2003), pp. 371–402.
- [31] ———, *The GLT class as a generalized Fourier analysis and applications*, Linear Algebra and its Applications, 419 (2006), pp. 180–233.
- [32] S. SERRA-CAPIZZANO AND P. TILLI, *Extreme singular values and eigenvalues of non-Hermitian block Toeplitz matrices*, Journal of Computational and Applied Mathematics, 108 (1999), pp. 113–130.
- [33] B. SHAPIRO AND F. ŠTAMPACH, *Non-self-adjoint Toeplitz matrices whose principal submatrices have real spectrum*, Constructive Approximation, 49 (2019), pp. 191–226.
- [34] R. SMITH, GENERICSCHUR.JL. <https://github.com/RalphAS/GenericSchur.jl>, 2023.
- [35] ———, PSEUDOSPECTRA.JL. <https://github.com/RalphAS/Pseudospectra.jl>, 2023.
- [36] G. SZEGŐ, *Beiträge zur Theorie der Toeplitzschen Formen*, Mathematische Zeitschrift, 6 (1920), pp. 167–202.
- [37] P. TILLI, *A note on the spectral distribution of Toeplitz matrices*, Linear and Multilinear Algebra, 45 (1998), pp. 147–159.
- [38] ———, *Some results on complex Toeplitz eigenvalues*, Journal of Mathematical Analysis and Applications, 239 (1999), pp. 390–401.
- [39] L. N. TREFETHEN AND M. EMBREE, *Spectra and pseudospectra*, Princeton University Press, Princeton, NJ, July 2005.
- [40] E. TYRTYSHNIKOV AND N. ZAMARASHKIN, *Spectra of multilevel Toeplitz matrices: Advanced theory via simple matrix relationships*, Linear Algebra and its Applications, 270 (1998), pp. 15–27.
- [41] E. V. EGERVÁRY AND O. SZÁSZ, *Einige extremalprobleme im bereiche der trigonometrischen polynome*, Mathematische Zeitschrift, 27 (1928), pp. 641–652.
- [42] T. G. WRIGHT, *EigTool*. <http://www.comlab.ox.ac.uk/pseudospectra/eigtool/>, 2002.

A Appendix: Algorithm

In this Appendix we present a full implementation of the proposed algorithm in this paper, to compute the full spectrum of $T_n(g_{r,s})$, assuming Conjecture 1 is true. The algorithm is written with clarity in mind, and not optimised for efficiency.

A.1 Setup and required packages

Required packages, and functions to construct square and rectangular Toeplitz matrices.

```
using LinearAlgebra
using GenericSchur # If using BigFloat (or other data types) instead of Float64
setprecision(BigFloat, 256) # If using BigFloat, choose a precision
# Toeplitz matrices of sizes n x n
function toeplitz(n::Integer, vc::Vector, vr::Vector, T::Type = Float64)
    Tn = zeros(T,n,n)
    for ii = 1:min(n,length(vc))
        Tn += vc[ii]*diagm(-ii+1=>ones(T,n-ii+1))
    end
    for jj = 2:min(n,length(vr))
        Tn += vr[jj]*diagm( jj-1=>ones(T,n-jj+1))
    end
    return Tn
end
# Rectangular Toeplitz matrices of sizes m x n
toeplitz(m::Integer, n::Integer, vc::Vector, vr::Vector, T::Type = Float64) =
    toeplitz(max(m,n), vc, vr, T)[1:m, 1:n]
```

A.2 Construct $B_{n_\sigma}^{n,r,s}$ matrices

```
function construct_B(n::Integer, r::Integer, s::Integer, T1::Type = Float64, T2::
Type = Int128; remove_corner::Bool = true)
     $\sigma$  = r+s
     $\beta_\sigma$  = mod(n, $\sigma$ )
     $n_\sigma$  = div(n, $\sigma$ )
    M, P = construct_M_P(r, s)
    B = I( $n_\sigma$ )
    m = M[ $\beta_\sigma$ +1,:]
    p = P[ $\beta_\sigma$ +1,:]
    for kk = 1:r
        if p[kk] >= 0
            B *= transpose(construct_shifted_Tncm( $n_\sigma$ ,m[kk],T2)) *
construct_shifted_Tncm( $n_\sigma$ ,1,T2)^(p[kk])
        else
            B *= convert.(T2, transpose(construct_shifted_Tncm( $n_\sigma$ ,m[kk],T2)) /
construct_shifted_Tncm( $n_\sigma$ ,1,T2))
        end
    end
    B = convert.(T1, B)
    # If beta>s and remove_corner is true, then extract corner from larger matrix
and remove it from B
    if  $\beta_\sigma$  > s && remove_corner
        B_large = construct_B( $\sigma^3 + \beta_\sigma$ , r, s, T1, T2, remove_corner = false)
         $n_{\min}$  = min(r-1,  $n_\sigma$ )
        corner = abs.(B_large[1: $n_{\min}$ , end+1- $n_{\min}$ :end])
        B[1: $n_{\min}$ , end+1- $n_{\min}$ :end] += (-1)^(isodd( $n_\sigma$ ))*corner
    end
    return B
end
```

A.3 Construct \mathcal{M} and \mathcal{P}

```
function construct_M_P(r::Integer, s::Integer)
    σ = r+s
    m_array = repeat(1:σ, inner=r)
    p_array = repeat(-1:s, inner=r)
    M = toeplitz(σ, r, m_array[r:r+σ-1], ones(Int64,r), Int64)
    P = toeplitz(σ, r, reverse(p_array[2:σ+1]), p_array[σ+1:σ+r], Int64)
    # If r > 1, permute columns
    if r != 1
        τ = mod(s, r)
        p_perm = mod.(τ:τ:r*τ, r)
        p_perm[end] = r
        M = M[:, p_perm]
        P = P[:, p_perm]
    end
    return M, P
end
```

A.4 Construct $T_n(e^{-i\theta}c(\theta)^m)$ matrices

```
function construct_shifted_Tncm(n::Integer, m::Integer, T::Type = Float64)
    v = binomial.(m,0:m)
    return toeplitz(n, v[2:end], reverse(v[1:2]), T)
end
```

A.5 Compute positive real eigenvalues $\lambda_+(T_n(g_{r,s}))$

```
function construct_positive_real_eigenvalues(n::Integer, r::Integer, s::Integer, T1
::Type = Float64, T2::Type = Int128)
    σ = r+s
    γ = gcd(r,s)
    σ_γ = div(σ, γ)
    β_γ = mod(n,γ)
    n_γ = div(n-β_γ,γ)
    r_γ = div(r,γ)
    s_γ = div(s,γ)
    # Trivial Case
    if n_γ < σ_γ
        n_γ_σ = div(n_γ,σ_γ)
        return repeat(zeros(T1, n_γ_σ), γ)
    end
    Bn_γ_σ = construct_B(n_γ,r_γ,s_γ,T1,T2)
    # Compute eigenvalues. If not using T1 = Float64, then it may be necessary to
    add a 'maxiter=100000' argument to eigvals
    eBn_γ_σ = real.(Complex.(eigvals(Bn_γ_σ)).^(convert(T1, 1)/σ_γ))
    if β_γ == 0
        return sort(repeat(eBn_γ_σ, γ))
    else
        Bn_γp1_σ = construct_B(n_γ+1,r_γ,s_γ,T1,T2)
        eBn_γp1_σ = real.(Complex.(eigvals(Bn_γp1_σ)).^(convert(T1, 1)/σ_γ))
        return sort(vcat(repeat(eBn_γ_σ, γ-β_γ), repeat(eBn_γp1_σ, β_γ)))
    end
end
```

A.6 Construct all eigenvalues $\lambda_j(T_n(g_{r,s}))$ for $j = 1, \dots, n$

```
function construct_all_eigenvalues(n::Integer, r::Integer, s::Integer, T1::Type =
Float64, T2::Type = Int128)
     $\sigma = r+s$ 
     $\gamma = \text{gcd}(r,s)$ 
     $\omega = \text{div}(\sigma,\gamma)$ 
    positive_real_eigenvalues = construct_positive_real_eigenvalues(n,r,s,T1,T2)
    rotations = exp.((0: $\omega-1$ )*2im*convert(T1,pi)/ $\omega$ )
     $\beta_\gamma = \text{mod}(n, \gamma)$ 
     $n_\gamma = \text{div}(n-\beta_\gamma, \gamma)$ 
     $n_0 = (\gamma-\beta_\gamma)*\text{mod}(n_\gamma,\omega) + \beta_\gamma*\text{mod}(n_\gamma+1,\omega)$ 
    return vcat(zeros(T1, n_0), kron(rotations, positive_real_eigenvalues))
end
```